Acquisition of Iron by Alkaliphilic *Bacillus* Species[▽]

Duncan G. G. McMillan,[1][¶] Imelda Velasquez,[3] Brook L. Nunn,[4] David R. Goodlett,[4]
Keith A. Hunter,[3] Iain Lamont,[2] Sylvia G. Sander,[3]* and Gregory M. Cook[1]*

*Department of Microbiology and Immunology,[1] Department of Biochemistry,[2] and Department of Chemistry,[3]
University of Otago, P.O. Box 56, Dunedin, New Zealand, and Medicinal Chemistry Department,
University of Washington, Box 358610, Seattle, Washington 98115[4]*

The biochemical and molecular mechanisms used by alkaliphilic bacteria to acquire iron are unknown. We demonstrate that alkaliphilic (pH > 9) *Bacillus* species are sensitive to artificial iron (Fe^{3+}) chelators and produce iron-chelating molecules. These alkaliphilic siderophores contain catechol and hydroxamate moieties, and their synthesis is stimulated by manganese(II) salts and suppressed by $FeCl_3$ addition. Purification and mass spectrometric characterization of the siderophore produced by *Caldalkalibacillus thermarum* failed to identify any matches to previously observed fragmentation spectra of known siderophores, suggesting a novel structure.

Iron is an abundant element in nature; however, in most aqueous aerobic environments iron forms insoluble ferric hydroxide, $Fe(OH)_3$. This poses a major problem for most aerobic bacteria, as ferric hydroxide has a solubility constant of 10^{-39} M, therefore limiting the concentration of ferric ions to 10^{-18} M at pH 7.0. For example, bacteria living in seawater (approximate pH 8.0) require iron, yet dissolved iron is only present at 0.02 to 2.0 nM (5). Despite this apparent lack of bioavailability, iron has been repeatedly demonstrated to be an essential element for aerobic bacterial growth (1).

With the lack of readily accessible iron at physiological pH, most bacteria have evolved systems to deal with the incumbent problem of iron acquisition. Under iron-rich conditions, Fe^{2+} uptake receptors, such as FeoAB, are synthesized in bacteria, which passively import iron in the immediate vicinity of the cell (1, 23). No equivalent system has been identified for Fe^{3+} transport. To acquire Fe^{3+} under aqueous aerobic conditions, bacteria commonly have import systems involving the synthesis, secretion, and regathering of a group of secondary metabolites known as siderophores (1, 11). Siderophores are low-molecular-weight chemical moieties that chelate Fe^{3+} and typically have complex formation (K_f) constants in the range of 10^{23} to 10^{52} (11). Siderophores, like other chelators, are known to increase the solubility of iron by hindering the formation of Fe-oxyhydroxides at high pH, at which the Fe-oxyhydroxides are the dominating inorganic species (27). Siderophores are also known to facilitate the dissolution of Fe from minerals (3). Siderophore-iron complexes can either be transported through cellular membranes using dedicated transport systems or if the Fe(III) central atom is reduced, making the iron bioavailable

for cellular processes (10, 14). Three major groups of siderophores have been described in bacteria: hydroxamates, catecholates, and carboxylates. Hydroxamates and catechols are commonly produced by aerobic bacteria living at neutral to alkaline pH, whereas carboxylates are significantly more common in bacteria living in mildly acidic pH (11–13). In the genus *Bacillus*, *Bacillus megaterium* and *Bacillus subtilis* are producers of schizokinen and bacillibactin, respectively (6, 20). *Bacillus anthracis* produces both a catechol and a hydroxamate siderophore (7, 34), and *B. licheniformis* strain VK21 is the only known example of a thermoresistant catecholate-producing Gram-positive bacterium (32).

Although there is extensive literature on iron capture mechanisms in bacteria that thrive at neutral pH, there is little information at a biochemical or molecular level on how aerobic bacteria growing at extreme alkaline pHs (i.e., pH 9 to 11) acquire iron. At alkaline pH, the solubility constant for iron decreases far below the requirement for living cells, and the concentration of bioavailable iron is estimated to be approximately 10^{-23} M at pH 10 (11). Taking this extreme lack of iron into account, the sequestering mechanisms of alkaliphilic bacteria must be powerful, yet there has been little analysis of the types of iron-chelating molecules these bacteria produce.

Alkaliphilic bacilli are sensitive to ethylenediamine *O*-hydroxyphenylacetic acid (EDDHA), but not 2,2′-dipyridyl. To examine the iron requirements of alkaliphilic bacteria, we tested four species of alkaliphilic *Bacillus* that have been studied in detail, and for most, genome sequences are available (Table 1). All strains were routinely grown in 50-ml flasks (1:5 headspace) containing alkaline basal medium (22): 0.5 g/liter $NaSO_4$, 0.1 g/liter $(NH_4)_2SO_4$, 0.1 g/liter $MgSO_4 \cdot 7H_2O$, 0.2 g/liter K_2HPO_4, 9.0 g/liter $NaHCO_3$, 2 g/liter Trypticase peptone (Becton-Dickinson), 5 ml of *Dictyoglomus* trace elements (25), and an appropriate carbon source where indicated. All strains were grown at their respective pH and temperature optima, and the final pH of the growth medium was ±0.5 pH units of the starting pH value (Table 1).

We studied the effects of increasing concentrations of the artificial iron chelators EDDHA (Sigma) and 2,2′-dipyridyl

* Corresponding author. Mailing address: Department of Microbiology and Immunology, University of Otago, P.O. Box 56, Dunedin, New Zealand. Phone: 64 3 479 7722. Fax: 64 3 479 8540. E-mail for G. M. Cook: gregory.cook@otago.ac.nz. E-mail for S. G. Sander: sylvias@chemistry.otago.ac.nz.
¶ Present address: Astbury Centre, Institute of Membrane and Systems Biology, Faculty of Biological Sciences, University of Leeds, Leeds LS2 9JT, United Kingdom.
▽ Published ahead of print on 27 August 2010.

TABLE 1. Growth characteristics of alkaliphilic bacteria used in this study

Alkaliphile	pH range	Optimum pH	Optimum temp (°C)	Reference
Caldalkalibacillus thermarum strain TA2.A1	7.5–10.5	9.5	65	22
Bacillus halodurans C-125	7.5–11.0	9.5	37	29
Bacillus alcalophilus DSM 485	8.5–12.0	10.0	37	33
Bacillus pseudofirmus OF4	7.5–11.0	9.5	30	30

(Sigma) on the aerobic growth of *Caldalkalibacillus thermarum*, *Bacillus halodurans*, *Bacillus pseudofirmus*, and *Bacillus alcalophilus* (Fig. 1). Cultures were grown overnight in alkaline basal medium, at the respective pH and temperature optima (Table 1), supplemented with 50 mM glutamate and various concentrations of either EDDHA or 2,2′-dipyridyl, and the final optical density (OD) was determined. All bacteria tested were sensitive to EDDHA at increasing concentrations (up to 500 μM) as observed by a decrease in the final OD at 600 (OD_{600}), expressed as a percentage of the final OD_{600} of untreated cultures (Fig. 1). The alkaliphilic bacilli investigated in this study were relatively insensitive to 2,2′-dipyridyl (Fig. 1). The lack of sensitivity of all strains to 2,2′-dipyridyl was not unexpected, as this compound is proposed to chelate ferrous ions (log stability constant, 17.6) (9), which are largely absent under aerobic conditions at alkaline pH (11). EDDHA chelates both ferrous and ferric ions, with log stability constants of 14.3 and 33.9, respectively (9).

In addition to iron binding, EDDHA is also known to bind other cations (e.g., magnesium binding has a log stability constant of 9.76) (35). To verify that the effect of EDDHA was iron specific, additional $MgCl_2$ or $FeCl_3$ was added to the growth medium. To place greater stress on the cells for iron, we grew the cells on succinate as the sole carbon source, a nonfermentable carbon source that is strictly coupled to oxidative phosphorylation. When *C. thermarum* was grown in medium containing succinate, EDDHA inhibited growth at 25 μM (Fig. 2A). The addition of $MgCl_2$ did not affect the sensitivity of *C. thermarum* to EDDHA, but with the addition of $FeCl_3$ it was able to overcome the inhibition by EDDHA. A similar trend was seen for the other alkaliphilic bacteria tested (Fig. 2B to D). Taken together, these data suggest that iron is an obligate growth requirement for the alkaliphilic bacteria examined in this study at their respective pH and temperature optima (Table 1). Many of the alkaliphiles tested in this study
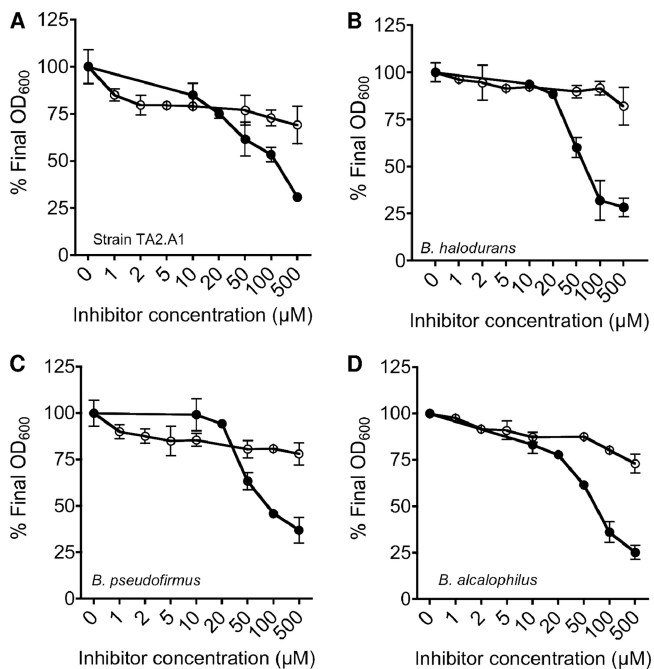

FIG. 1. Effects of either EDDHA (closed circles) or 2,2′-dipyridyl (open circles) on the growth of alkaliphilic bacteria. (A) *C. thermarum* (strain TA2.A1); (B) *B. halodurans*; (C) *B. pseudofirmus*; (D) *B. alcalophilus*. All cultures were grown for 24 to 26 h in alkaline basal medium, supplemented with 50 mM glutamate, at the optimum pH and temperature for each strain, and the final OD_{600} was recorded. The values are expressed as the optical density obtained in the absence of iron chelator (nominally 100%) compared to the optical density obtained in the presence of iron chelator (0 to 100%). All values are the means of two biological replicate experiments, and the standard errors of the means are shown.
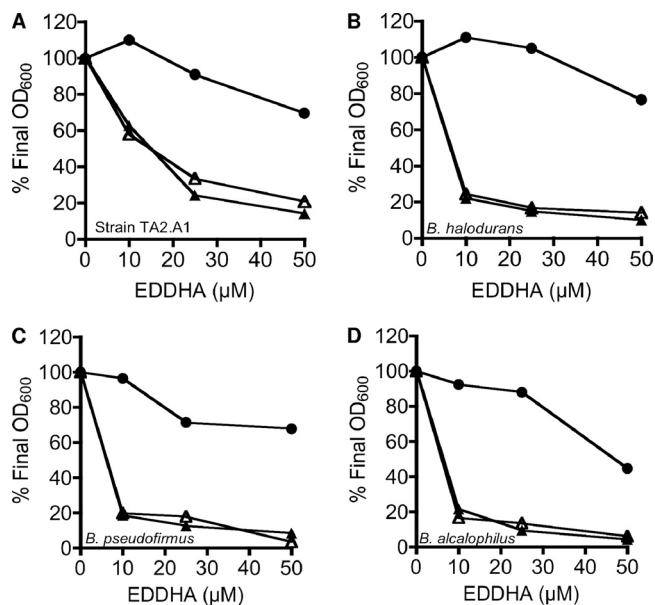

FIG. 2. Effects of EDDHA on the growth of alkaliphilic bacteria. (A) *C. thermarum* (strain TA2.A1); (B) *B. haloduran*; (C) *B. pseudofirmus*; (D) *B. alcalophilus*. All cultures were grown for 24 to 26 h in alkaline basal medium supplemented with 50 mM succinate, at the optimum pH and temperature for each strain, and the final OD_{600} was recorded. The growth medium was supplemented with EDDHA (10 to 50 μM) in the absence of $FeCl_3$ and $MgCl_2$ (closed triangles), in the presence of 150 μM $FeCl_3$ (closed circles), or in the presence of 150 μM $MgCl_2$ (open triangles). Representative data from replicate experiments are shown.
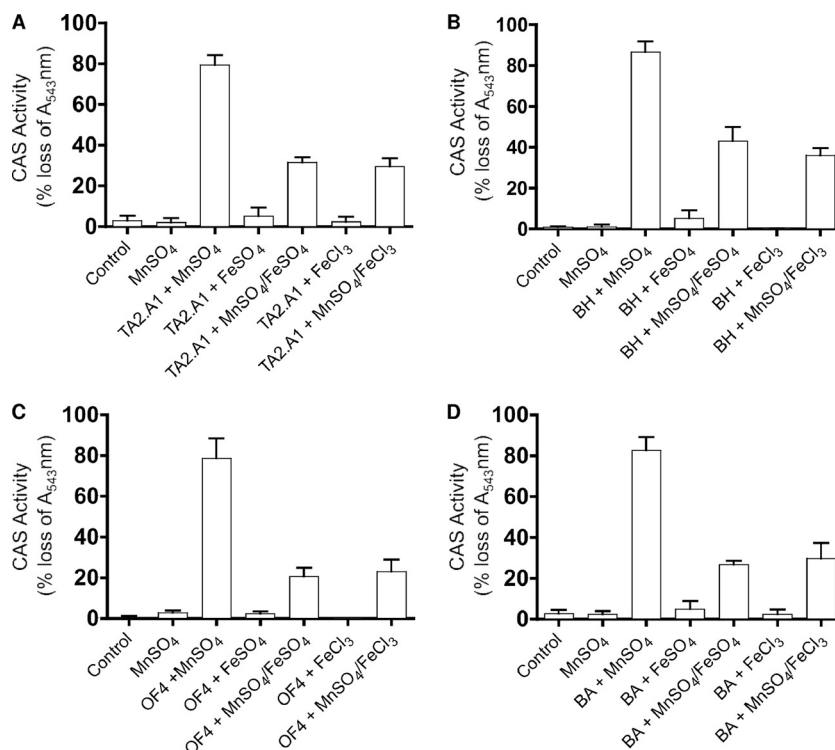
FIG. 3. Effects of manganese and iron on siderophore production by alkaliphilic *Bacillus* species. (A) *C. thermarum* (TA2.A1); (B) *B. halodurans* (BH); (C) *B. pseudofirmus* (OF4); (D) *B. alcalophilus* (BA). Growth medium was supplemented as indicated with the following: 60 μM $MnSO_4$, 2.5 μM $FeSO_4$, 2.5 μM $FeCl_3$, 60 μM $MnSO_4$ plus 2.5 μM $FeSO_4$, or 60 μM $MnSO_4$ plus 2.5 μM $FeCl_3$. The controls were uninoculated growth medium with or without 60 μM $MnSO_4$. All cultures were grown for 3 to 4 days in alkaline basal medium at the optimum pH and temperature for each strain and supplemented with 50 mM succinate, and the CAS assay was performed on cell-free culture supernatants. The values reported are expressed as the percent loss in absorbance at 543 nm (CAS activity); the means of two biological replicate experiments and the standard errors of these determinations are shown.

are facultative, i.e., able to grow over a broad pH range, and it remains to be investigated what effects iron-chelating agents have on the growth of these bacteria at near-neutral pH values.

Siderophore production by aerobic alkaliphilic bacteria. Temirov et al. (32) reported that the addition of manganese(II) salts to growth medium dramatically increased the secretion of a catecholic (Fe^{3+}) siderophore by *Bacillus licheniformis* strain VK21. The chrome azurol S (CAS) assay, a common diagnostic test for siderophore production (26), was used to determine if an iron-chelating metabolite was produced in liquid culture medium. This determination was carried out on culture supernatant (typically 50-ml cultures) that was neutralized to pH 6.5 by using 0.2 M HCl. The supernatant was added to CAS solution in a 1:1 ratio and incubated for 2 h. Absorbance was measured as the OD_{543} upon reaction completion (26). The effect of $MnSO_4$ addition to the growth medium of all alkaliphilic *Bacillus* species on siderophore production, as monitored with the CAS reagent, was tested (Fig. 3). The results are expressed as the percentage loss of absorbance at 543 nm (i.e., decolorization of the blue CAS dye to orange, indicating the presence of siderophores, iron-chelating compounds) compared to the blank medium control. When either the uninoculated growth medium with or without manganese(II) salts was tested for iron-chelating agents, there was little change in the absorbance at 543 nm (Fig. 3). If manganese(II) salts were included in the inoculated growth medium,

all bacteria showed an increase in the synthesis of iron-binding molecules, which could be suppressed by the addition of additional iron ($FeSO_4$ or $FeCl_3$) (Fig. 3). These data indicated the production of iron-binding molecules by alkaliphilic bacteria.

Siderophores fall into a number of classes based on the chemical composition of their functional groups for iron binding. The presence of these groups is the basis for many assays designed to detect siderophores. The CAS assay does not differentiate between these different functional groups. All strains were screened for their ability to synthesize siderophores in assays that targeted the chemical structures for catecholates and hydroxymates (Table 2). The presence of catecholic compounds in cell-free culture supernatants from all strains was examined using a colorimetric reaction with ammonium-iron citrate and 1,10-phenanthroline (24). This reaction is specific to aromatic compounds containing vicinal hydroxyl groups (24). Based on this assay, *C. thermarum*, *B. alcalophilus*, and *B. pseudofirmus* cultures were all positive for the presence of a catecholic metabolite (Table 2). This was confirmed further by determining the UV_{254} fluorescence properties exhibited by catecholic metabolites and quenching of this fluorescence with iron (Table 2). The production of catecholate-type siderophores by alkaliphilic bacteria is consistent with growth at alkaline pH, as catechols have been shown to dissociate at pH 9 to 10, while hydroxamates and carboxylates dissociate at lower pH values (8 to 9 and 3.5 to 5, respec-

TABLE 2. Characterization of iron-binding metabolites in culture supernatants of alkaliphilic bacteria

| Test strain | Siderophore detection method[a] | | | | | |
| | Catecholate | | Hydroxamate | | UV$_{254}$ fluorescence | |
	$-Mn^{2+}$	$+Mn^{2+}$	$-Mn^{2+}$	$+Mn^{2+}$	$-Fe^{3+}$	$+Fe^{3+}$
C. thermarum	+	+++	−	++	+++	−
B. halodurans	−	−	+	+++	−	−
B. alcalophilus	+	+++	−	−	+++	−
B. pseudofirmus	+	+++	−	−	+++	−

[a] Catecholic metabolites were detected using the ammonium-iron citrate test (24); hydroxamate metabolites were detected using the modified Csaky test (16). Catecholic metabolites were also detected by Fe^{3+}-quenchable UV$_{254}$ fluorescence. All cultures were grown in either the presence (+) or absence (−) of 60 μM MnSO$_4$. All tests were quantified against a concentration curve for purified pyoverdine. +, concentration of the iron-binding metabolite was 0 to 0.1 μg/ml; ++, concentration of the iron-binding metabolite was 0.1 to 1.0 μg/ml; +++, concentration of the iron-binding metabolite was 1.0 to 10.0 μg/ml; −, concentration of the iron-binding metabolite was below the detection limit.

tively) (11). The one exception to this rule was *B. halodurans*, which according to the published genome (31) has similar nonribosomal peptide synthase (NRPS) genes as those required to encode aerobactin, a hydroxamate siderophore (4).

Neutralized cell-free culture supernatants of *C. thermarum*, *B. halodurans*, *B. pseudofirmus*, and *B. alcalophilus* were examined for the presence of hydroxamates by using the modified Csaky assay (16). Both *C. thermarum* and *B. halodurans* supernatants gave a positive reaction for this test, suggesting that they produced a siderophore containing at least one hydroxamate moiety (Table 2). *B. pseudofirmus* and *B. alcalophilus* supernatants did not yield a positive result, suggesting that these bacteria do not produce a hydroxamate-type siderophore (Table 2).

Purification and characterization of siderophores from *C. thermarum*. The initial tests performed suggested that alkaliphilic *Bacillus* species produce iron-chelating molecules. Under conditions of either excess manganese(II) salts or EDDHA in alkaline basal medium (22), it was observed that *C. thermarum* produced an orange pigment. Bacterial iron-bound siderophores are reported to be yellow-brown to red-brown in color (11), and it was hypothesized that this material was an iron-bound siderophore. The pigment (siderophore) produced by *C. thermarum* was extracted from the culture supernatant based on published methods (8, 18, 28). In brief, culture supernatant (pH 9; 750 ml) was transferred into a separating funnel, acidified with quartz-distilled HCl to pH 2.7, and extracted with 100 ml of ethyl acetate. The bottom aqueous layer was discarded, while the top ethyl acetate layer containing the siderophore fraction was collected. This procedure was repeated in total three times. A second extraction with 75 ml of 10% (wt/vol) sodium hydrogen carbonate was performed twice; the aqueous bottom layer was again discarded, while the ethyl acetate layer was retained. The pooled organic phase was transferred into an acid-cleaned high-density polyethylene (HDPE) bottle and dried over sodium sulfate (10 g) at 4°C overnight. The organic phase was filtered through 0.45-μm polytetrafluoroethylene (PTFE) syringe filter (Sartorius Minisart) and evaporated to dryness using a rotary evaporator. The resulting red residue was dissolved with acidified (pH 1) deionized water (>18 MΩ; MQH$_2$O; Millipore) in an ultrasonic bath.

Solid-phase extraction of the siderophore fraction was completed on a 50-ml column (laboratory prepared) containing 40 g XAD-16 (Sigma). The siderophore extract was slowly transferred onto the XAD-16 column, which was precleaned with 100% methanol (MeOH), followed by acidified MQH$_2$O (pH 1), and rinsed thoroughly with MQH$_2$O. The compounds that bound to the resin were eluted with four bed volumes of 100% methanol (high-performance liquid chromatography [HPLC] grade; Merck). The volume was reduced to ~10 ml by using a rotary evaporator at <30°C. This solution was then transferred to a 15-ml test tube and evaporated to dryness using a SAVANT Speedvac Plus SC210A. The resulting siderophore-containing residue was stored frozen at −20°C.

At the end of each step in purification, siderophore characterization assays were performed to track activity. The Arnow test was performed by adding equal volumes of 0.5 N HCl, nitrite-molybdate reagent, and 1 N NaOH to the eluent (2). Methanol was used as a blank for all assays. The fractions containing siderophore were spotted (5 and 10 μl) onto an Alugram SIL G/UV254 0.2-mm-thick silica 60 aluminum-backed thin-layer chromatography (TLC) plate with built-in UV$_{254}$ indicator dye. Prior to use, the plates were developed with methanol and air dried for 30 min. Isopropanol-methanol-glacial acetic acid-water (7.5:1:1:0.5, vol/vol/vol/vol) was used as the mobile phase, and the developing tank was conditioned for 30 min before the plate was developed. After development, the plates were air dried and analyzed under UV$_{254}$. A single spot was observed as light orange in white light and as blue under UV light, with a retention factor (RF) value of 0.77 (Fig. 4).

Prior to mass spectrometry (MS) analyses, the siderophore-containing sample was redissolved in 250 μl of 50% methanol. Methanol was removed using the speedvac, and methanol and trifluoroacetic acid (TFA) were added to yield a final solution of 5% methanol, 0.1% TFA. For desalting and further purification of the siderophore, we performed a sequential extraction with increasing methanol/water ratios (i.e., 10%, 20%, 30%, and 70%) using an Ultra microspin C$_{18}$ column (Vydac; catalog number 8818V, Nest Group Inc.). Care was taken to ensure that no wash solution was carried over to the next step. New vials were used for each of the fractionation steps. The red-orange pigment, indicative of an iron-bound siderophore, eluted from the column with the 20% MeOH fraction.

Final chromatographic separations and mass spectrometry analyses were performed on a NanoAcquity HPLC system (Waters Corp., Milford, MA) attached to a hybrid linear ion trap-orbitrap mass spectrometer (LTQ-OT; ThermoFisher, San Jose, CA). All capillary columns for HPLC separations
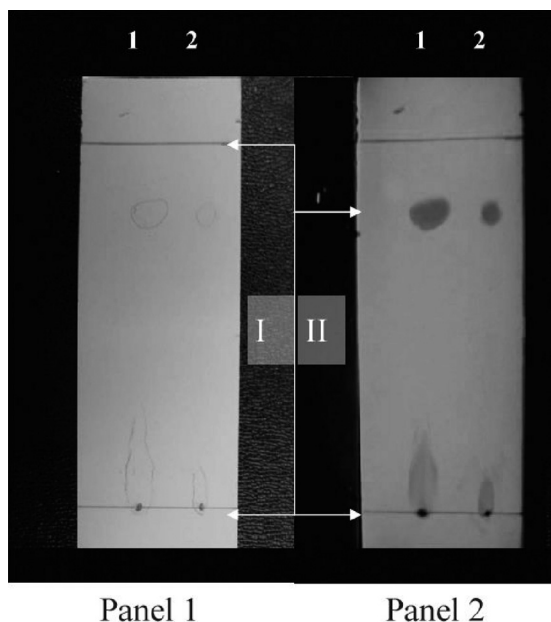
FIG. 4. TLC of XAD-16 eluate. XAD-16 eluate was spotted onto an Alugram SIL G/UV254 0.2-mm-thick silica 60 aluminum-backed TLC plate with built-in UV_{254} indicator dye in 10-μl (lane 1) or 5-μl (lane 2) increments. TLC was conducted using a isopropanol-methanol-glacial acetic acid-water (7.5:1:1:0.5) mobile phase. The solvent front distance from the origin is indicated by I, and the distance the spot traveled is indicated by II. Panels 1 and 2 are the same TLC plate visualized under white light and UV light, respectively.

were made in-house with silica tubing. Siderophores were first trapped on a 100-μm inner diameter (i.d.), 20-mm-long precolumn packed with 200-Å, 5-μm Magic C_{18} particles (Michrom), followed by separation on a gravity-pulled 75-μm i.d., 120-mm-long analytical column packed with 100-Å, 5-μm Magic C_{18} particles. Chromatography was performed using a mobile phase consisting of (A) water, 0.1% (vol/vol) formic acid and (B) ACN, 0.1% (vol/vol) formic acid. Siderophore samples were loaded onto the precolumn in an A:B ratio of 95:5 (4 μl/min for 7 min) and subsequently separated on the analytical column (250 nl/min). The programmed gradient was as follows: 0 min with A (95%), B (5%); 55 min with A (65%), B (35%); 60 min with A (15%), B (85%); 65 min with A (5%), B (95%); 75 to 95 min with A (95%), B (5%). Concentrations of the samples were incrementally increased for each injection to achieve a total ion current of >1E7. The LTQ-OT was run in the positive ion mode, in which electrospray voltage was applied using a micro-T-junction with a gold wire in contact with the liquid between the precolumn and analytical column. Several siderophore standards were analyzed after tuning and calibrating the instrument (capillary temperature, 275°C; collision energy [CE], 45%). Since the structures of siderophores produced by *C. thermarum* are unknown, we optimized the instrument to observe either the +2 or +1 charge state of all four standards (enterobactin, desferrioxamine, ferrichrome, and pyoverdine). Capillary temperature and voltage were optimized to 325°C and 44 V, respectively. These settings provided either the $[M + H]^+$ or $[M + 2H]^{2+}$ ions for the four siderophore standards. Tuning was performed on the $[M + 2H]^{2+}$ ion of a pyoverdine standard. MS survey scans were completed using the orbitrap (*m/z* 200 to 2,000) with a mass accuracy at or below 2 ppm. Using a data-dependent strategy (21), the five most intense ions were selected for collision-induced dissociation (CID) in the LTQ (CE, 45%). Tandem mass spectra collected in the LTQ achieved a mass accuracy of 50 to 100 ppm. Only ions with a +1, +2, or unassigned charge state were selected for fragmentations. Prior to the analysis of the *C. thermarum* siderophore, enterobactin, desferrioxamine, and pyoverdine standards were analyzed using the above parameters and identical tune file. Direct infusion of a mixed pyoverdine and enterobactin standard yielded the $[M + H]^+$ and $[M + 2H]^{2+}$ pyoverdine ions and enterobactin Na^+ and enterobactin K^+ ions. To ensure there was no column carryover from the analysis of siderophore standards, new analytical and precolumns were installed for the analysis of *C. thermarum* samples. Angiotensin II peptide (DRVYIHPF) was intermittently used as an internal standard to check the mass accuracy of the precursor ions in the orbitrap and ensure consistency. Full-gradient blanks (90 min) were completed between the samples in order to clean and condition the column. At the end of the analysis sequence, the mass accuracy of a 100-pg enterobactin standard was determined to be below 2 ppm in the orbitrap.

C. thermarum siderophore extracts were spiked with $FeSO_4$ to ensure most siderophore species present were bound to iron. The theoretical natural ratio of ^{56}Fe to ^{54}Fe (100:6) provided a unique signature to search the MS1 spectra. Each mass that demonstrated the approximate iron isotope signature was investigated. Potential masses were rejected as possible siderophores if the mass was present in (i) a repeating ion series, (ii) a blank, or (iii) blanks with $FeSO_4$. Importantly, although over 10,000 MS1 data scans from all fractions were investigated to identify the unique iron isotope ratio of ^{56}Fe to ^{54}Fe (100:6) separated by 2 Da, as evidence for Fe-bound compounds, the pattern was only found in the mass spectrometry analyses from the red 20% MeOH fraction (Fig. 5). MS data from other MeOH fractions (10%, 30%, and 70% MeOH) exhibited no iron isotope patterns in the MS1 scans, demonstrating that the pigmented portion of the extract eluted in the same fraction as the organic compounds binding to iron. Once the protonated ferri-siderophore complex $[M + H]^+$ (*m/z* 597) was identified by the unique iron isotopic pattern, the mass of interest was searched for in blanks with and without iron additions to ensure that the unique mass distribution was not a result of iron-bound contaminants. The siderophore eluted off the C_{18} column at 58.6 min, yielding the characteristic iron isotopic pattern and providing a $[M + H]^+$ of *m/z* 597.27 (Fig. 5A and B). The primary ion resulting from the fragmentation of *m/z* 597.27 was *m/z* 301, which retained the bound iron. A fragment ion was also present at 297, which does not correspond with the iron isotopic pattern and suggests that this siderophore nearly fragments in half, yielding the two fragment ions of *m/z* 301 and 297. Both fragment ions *m/z* 301 and 297 were present in both the precursor scan and in the tandem mass spectra, suggesting that this siderophore is unstable and either fragmenting in solution and coeluting or fragmenting as the siderophore is introduced to the mass spectrometer via electrospray. As a result of the apparent nonstable structure of the *C. thermarum* 596 (TA2$_{596}$) in solution, we observed that many of the fragment ions resulting from
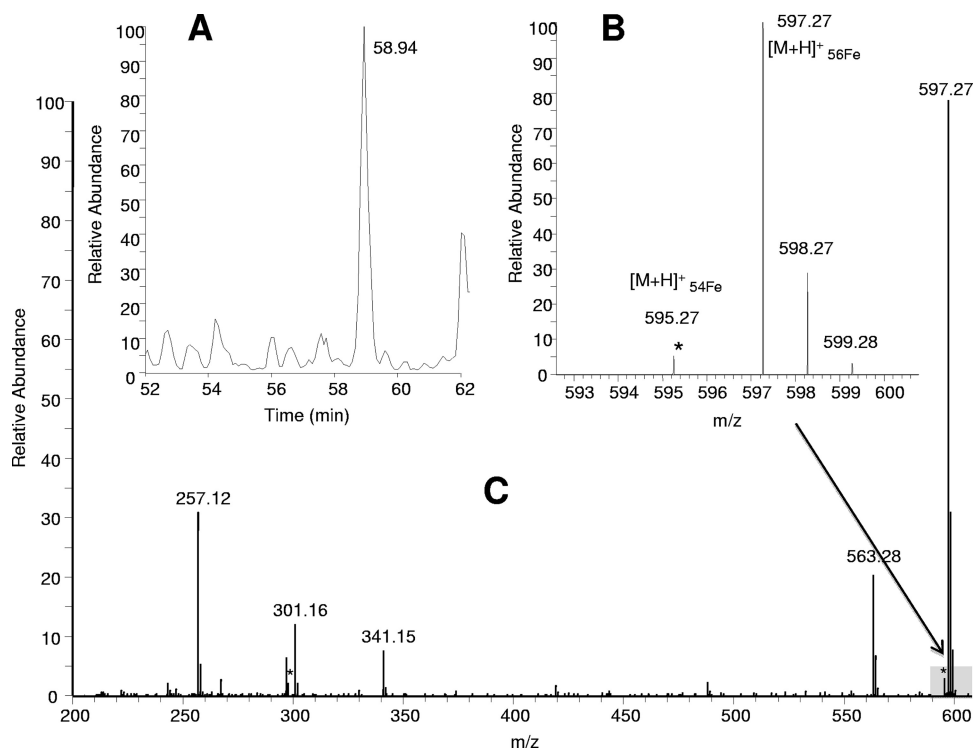
FIG. 5. (A) The observed chromatographic peak retaining all iron-bound siderophore fragments; (B) graph using a smaller scale of the [M + H]$^+$ results, showing the Fe-isotopic pattern observed; (C) precursor mass spectrum collected in the orbitrap Fe(III)-siderophore complex, with a molecular ion peak [M + H]$^+$ at m/z 597.

CID of TA2$_{596}$ (Table 3, m/z 301, 257, and 297) individually eluted from the chromatography column at the same time (58 min), providing additional fragmentation spectra (Table 3). Several studies examining siderophores in solution using HPLC in-line with electrospray-based mass spectrometry have noted that siderophores can have unstable structures when evaluated under acidic conditions, as is typically done prior to analysis on reverse-phase LC-tandem MS platforms (15, 17, 19). The tandem mass spectra collected on these in-solution fragments, in effect, provided excellent multistage tandem mass spectra, or simulated MS3. In addition, because these fragments were observed in the orbitrap during the precursor scan, higher-mass accuracy data were collected on these fragments. Fragment ions resulting from the fragmentation of TA$_{596}$ included m/z 301, 341, and 257, each of which retained iron and exhibited iron isotopic patterns. The behavior of these

ions illustrates strong affinity to Fe, which is a typical characteristic of siderophore-type compounds. Neutral losses of 18 Da, 17 Da, 44 Da, 28 Da, and 56 Da were observed. These resulted from common losses of H_2O, NH_3, $CONH_2$, CO, and C_4H_8, which are frequently observed during the fragmentation of siderophores. Large neutral losses that created the primary fragment ions, such as 256 Da and 296 Da, were searched for extensively in previously published fragmentation spectra of known siderophores (15, 17, 19). None of the large neutral losses, nor the resulting fragment ions observed from the fragmentation of TA2$_{596}$, has been previously observed.

In summary, all alkaliphilic bacteria in this study had an obligate requirement for iron at their respective growth pH and temperature optima, based on their sensitivity to the artificial iron chelator EDDHA. The CAS assay confirmed the production of iron-chelating metabolites in liquid culture medium and that manganese(II) salt addition enhanced this production, whereas iron addition suppressed this expression. Further chemical tests based on known siderophore functional groups suggested the production of catechol-type siderophores by *C. thermarum*, *B. alcalophilus*, and *B. pseudofirmus*, and this was further confirmed using the UV$_{254}$ fluorescence properties exhibited by catecholic metabolites and quenching of this fluorescence with iron. *C. thermarum* and *B. halodurans* produced a siderophore containing at least one hydroxamate moiety. Purification and mass spectrometric characterization of the siderophore produced by *C. thermarum* confirmed that this alkaliphilic bacterium synthesizes a novel siderophore containing at least one hydroxamate group that is iron bound and has

TABLE 3. Retention times and m/z ratios of TA2$_{596}$ precursor ions measured in the OT and fragment ions measured in the LTQ^a

Retention time in TA2$_{596}$ (min)	Precursor ion scan in OT (m/z)	Fragment ion scan in LTQ (m/z)
58.6	597.27*	301*, 257*, 341*, 297, 553
58.7	301.17*	257*, 245*, 284, 273, 132
34.5	257.13*	132*, 211*, 229, 239
58.3	297.16	280, 240, 269

^{a} Masses with a * indicate that the iron isotopic pattern was observed in either the precursor scan or the tandem mass spectrum. Underlined fragment masses are indicative of ions where tandem mass spectra were collected as a result of the primary siderophore, TA2$_{596}$, fragmenting prior to entering the collision cell.

a protonated *m/z* of 597.27. However, based on the Rioux test, there may also be one or more 3,4-dihydroxybenzoic acid residue functional groups in the structure, indicating there may be only one siderophore that has both catecholate and hydroxamate functional groups. *C. thermarum* grows at extremes of both pH and temperature, and the novel siderophore produced by this bacterium may reflect an adaptation to thermophilic temperatures and high pH. This remains to be investigated in other thermoalkaliphilic aerobic bacteria. Future work will focus on the isolation and structural identification of the siderophore, the identification of biosynthetic pathways utilized to make this siderophore, and the regulatory elements that control expression in response to iron.

REFERENCES

1. **Andrews, S. C., A. K. Robinson, and F. Rodriguez-Quinones.** 2003. Bacterial iron homeostasis. FEMS Microbiol. Rev. **27:**215–237.
2. **Arnow, E.** 1936. Colorimetric determination of the components of 3,4-dihydroxyphenylalanine-tyrosine mixtures. J. Biol. Chem. **118:**531–537.
3. **Brantley, S. L., L. J. Liermann, R. L. Guynn, A. Anbar, G. A. Icopini, and J. Barling.** 2004. Fe isotopic fractionation during mineral dissolution with and without bacteria. Geochim. Cosmochim. Acta **68:**3189–3204.
4. **Braun, V.** 1981. *Escherichia coli* cells containing the plasmid ColV produce the iron ionophore aerobactin. FEMS Microbiol. Lett. **11:**225–228.
5. **Bruland, K. W., K. J. Orions, and J. P. Cowens.** 1994. Reactive trace metals in the stratified central North Pacific. Geochim. Cosmochim. Acta **58:**3171–3182.
6. **Byers, B. R., M. V. Powell, and C. E. Lankford.** 1967. Iron-chelating hydroxamic acid (schizokinen) active in initiation of cell division in *Bacillus megaterium*. J. Bacteriol. **93:**286–294.
7. **Cendrowski, S., W. MacArthur, and P. Hanna.** 2004. *Bacillus anthracis* requires siderophore biosynthesis for growth in macrophages and mouse virulence. Mol. Microbiol. **51:**407–417.
8. **Chung Chun Lam, C. K., T. D. Jickells, D. J. Richardson, and D. A. Russell.** 2006. Fluorescence-based siderophore biosensor for the determination of bioavailable iron in oceanic waters. Anal. Chem. **78:**5040–5045.
9. **Dawson, R. M. C., D. C. Elliot, W. H. Elliot, and K. M. Jones.** 1986. Data for biochemical research. Clarendon Press, Oxford, England.
10. **Dhungana, S., and A. L. Crumbliss.** 2005. Coordination chemistry and redox processes in siderophore-mediated iron transport. Geomicrobiol. J. **22:**87–98.
11. **Drechsel, H., and G. Jung.** 1998. Peptide siderophores. J. Pept. Sci. **4:**147–181.
12. **Drechsel, H., G. Jung, and G. Winklemann.** 1992. Steriochemical characterization of rhizoferrin and identification of its dehydration products. Biometals **5:**141–148.
13. **Drechsel, H., M. Tschierske, A. Thieken, G. Jung, H. Zahner, and G. Winklemann.** 1995. The carboxylate siderophore rhizoferrin and its analogs produced by directed fermentation. J. Ind. Microbiol. **14:**105–112.
14. **Emery, T.** 1987. Reductive mechanism of iron assimilation, p. 235–250. *In* G. Winkleman, D. van der Helm, and J. B. Neilands (ed.), Iron transport in microbes, plants and animals. VCH, Weinheim, Germany.
15. **Feistner, G. J., D. C. Stahi, and A. H. Gabrik.** 1993. Proferrioxamine siderophores of *Erwinia amylovora*. A capillary liquid chromatography/electrospray tandem mass spectrometric study. Org. Mass Spectrom. **28:**163–175.
16. **Gillam, A. H., A. G. Lewis, and R. J. Anderson.** 1981. Quantitative determination of hydroxamic acids. Anal. Biochem. **53:**841–844.
17. **Gledhill, M.** 2001. Electrospray ionization-mass spectrometry of hydroxamate siderophores. Analyst **126:**1359–1362.
18. **Jacobs, A., G. P. White, and G. P. Tait.** 1977. Iron chelation in cell cultures by two conjugates of 2,3-dihydroxybenzoic acid (2,3-DHB). Biochem. Biophys. Res. Commun. **74:**1626–1630.
19. **Mawji, E., M. Gledhill, P. J. Worsfold, and E. P. Achterberg.** 2008. Collision-induced dissociation of three groups of hydroxamate siderophores: ferrioxamines, ferrichromes and coprogens/fusigens. Rapid Commun. Mass Spectrom. **22:**2195–2202.
20. **May, J. J., T. M. Wendrich, and M. A. Marahiel.** 2001. The *dhb* operon of *Bacillus subtilis* encodes the biosynthetic template for the catecholic siderophore 2,3-dihydroxybenzoate-glycine-threonine trimeric ester bacillibactin. J. Biol. Chem. **276:**7209–7217.
21. **McLafferty, F. W., and F. Turecek.** 1993. Interpretation of mass spectra, 4th ed. University Science Books, Mill Valley, CA.
22. **McMillan, D. G., S. Keis, M. Berney, and G. M. Cook.** 2009. Nonfermentative thermoalkaliphilic growth is restricted to alkaline environments. Appl. Environ. Microbiol. **75:**7649–7654.
23. **Ollinger, J., K. Song, H. Antelmann, M. Hecker, and J. D. Helmann.** 2006. Role of the Fur regulon in iron transport in *Bacillus subtilis*. J. Bacteriol. **188:**3664–3673.
24. **Rioux, C., C. D. Jordan, and J. B. M. Rattray.** 1983. Colorimetric determination of catechol siderophores in microbial cultures. Anal. Biochem. **133:**163–169.
25. **Sakai, T., K. Kobayashi, K. Kawagoe, and T. Beppu.** 1985. *Dictyglomus thermophilum* gen. nov., a chemoorganotrophic, anaerobic thermophilic bacterium. Int. J. Syst. Bacteriol. **35:**253–259.
26. **Schwyn, B., and J. B. Neilands.** 1987. Universal chemical assay for the detection and determination of siderophores. Anal. Biochem. **160:**47–56.
27. **Sunda, W., and S. Huntsman.** 2003. Effect of pH, light, and temperature on Fe-EDTA chelation and Fe hydrolysis in seawater. Mar. Chem. **84:**35–47.
28. **Tait, G. H.** 1975. The identification and biosynthesis of siderochromes formed by *Micrococcus denitrificans*. Biochem. J. **146:**191–204.
29. **Takami, H., and Horikoshi.** 1999. Reidentification of facultatively alkaliphilic *Bacillus* sp. C-125 to *Bacillus halodurans*. Biosci. Biotechnol. Biochem. **63:**943–945.
30. **Takami, H., and T. A. Krulwich.** 2000. Reidentification of facultatively alkaliphilic *Bacillus firmus* OF4 as *Bacillus pseudofirmus* OF4. Extremophiles **4:**19–22.
31. **Takami, H., K. Nakasone, Y. Takaki, G. Maeno, R. Sasaki, N. Masui, F. Fuji, C. Hirama, Y. Nakamura, N. Ogasawara, S. Kuhara, and K. Horikoshi.** 2000. Complete genome sequence of the alkaliphilic bacterium *Bacillus halodurans* and genomic sequence comparisons with *Bacillus subtilis*. Nucleic Acids Res. **28:**4317–4331.
32. **Temirov, Y. V., T. Z. Esikova, I. A. Kashparov, T. A. Balashova, L. M. Vinokurov, and Y. B. Alakhov.** 2003. A catecholic siderophore produced by the thermoresistant *Bacillus licheniformis* VK21 strain. Russ. J. Bioorg. Chem. **29:**542–549.
33. **Vedder, A.** 1934. *Bacillus alcalophilus* n. sp.; benevens enkele ervaringen met sterk alcalische voedingsbodems. Antonie Van Leeuwenhoek J. Microbiol. Serol. **1:**143–147.
34. **Wilson, M. K., R. J. Abergel, J. E. Arceneaux, K. N. Raymond, and B. R. Byers.** 2010. Temporal production of the two *Bacillus anthracis* siderophores, petrobactin and bacillibactin. Biometals **23:**129–134.
35. **Yunta, F., S. Garcia-Marco, J. J. Lucena, M. Gomez-Gallego, R. Alcazar, and M. A. Sierra.** 2003. Chelating agents related to ethylenediamine bis (2-hydroxyphenyl) acetic acid (EDDHA). Inorg. Chem. **42:**5412–5421.